RSC Advances

PAPER

View Article Online
View Journal | View Issue

Cite this: *RSC Adv.*, 2017, **7**, 49985

Fenton degradation of 4-chlorophenol using H_2O_2 *in situ* generated by Zn-CNTs/O_2 system

Yong Liu,[ab] Yanlan Liu,[a] Zhao Yang[a] and Jianlong Wang*[bc]

In this study, Zn-CNT composites were prepared by the infiltration fusion method and characterized by TEM, XPS and N_2 adsorption/desorption experiments. The reaction of Zn-CNTs and O_2 in aqueous solution was performed for the *in situ* generation of H_2O_2, which was employed to react with Fe^{2+} for the Fenton degradation of 4-chlorophenol (4-CP). The effect of various parameters, including the initial pH, dosage of Zn-CNTs and Fe^{2+} concentration on 4-CP degradation was examined. The removal efficiencies of 4-CP and TOC (total organic carbon) were 98.8% and 87.4%, respectively, when the Fe^{2+} concentration was 20 mg L^{-1}, initial pH was 2.0, Zn-CNT dosage was 2 g L^{-1}, reaction time was 20 min and O_2 flow rate was 400 mL min^{-1}. When 4-CP was spiked in the secondary effluent of a municipal wastewater treatment plant, the removal efficiency of 4-CP and TOC was 47.0% and 45.6%, respectively, under the above-mentioned conditions. The intermediate products were detected by LC-MS and IC, and the possible degradation pathway of 4-CP and the reaction mechanism of the Zn-CNTs/O_2/Fe^{2+} system were tentatively proposed.

Received 4th August 2017
Accepted 16th October 2017

DOI: 10.1039/c7ra08634b

rsc.li/rsc-advances

1. Introduction

The advanced oxidation processes (AOPs) based on the generation of hydroxyl radicals (˙OH) are excellent alternatives for the efficient removal of persistent organic pollutants.[1,2] Among all the AOPs, the Fenton process has been widely implemented due to its simplicity and the use of environmentally iron-based catalysts.[3] During the conventional Fenton process, H_2O_2 is usually provided by bulk feeding, which does not yield a high efficiency and has safety hazards associated with the chemical performance of H_2O_2. Recently, the Fenton process with the *in situ* generation of H_2O_2 has been extensively studied for the destruction of organic pollutants. One of the advantages of the *in situ* generation of H_2O_2 is that the H_2O_2 can be consumed at an appreciable controlled rate prior to decomposition into H_2O and O_2, which leads to an improved performance of H_2O_2 in the favored reaction direction.[4] Moreover, the application of *in situ* generated H_2O_2 has been found to be potentially safer and more economical than that of bulk commercial H_2O_2.[5] Various methods have been used for the *in situ* generation of H_2O_2 for the Fenton oxidation of organic pollutants, such as electro-Fenton,[6–8] photo-Fenton,[9,10] and bio-Fenton processes[11,12] *etc.* However, these processes require the use of a high concentration of electrolyte or electrical energy or luminous energy or nutrient substances, which limits their application in wastewater treatment.

The *in situ* generation of H_2O_2 can be obtained by a micro-electrolysis (ME) process based on the electrochemical reaction between O_2 and the ME materials, which was confirmed by the reduction of O_2 on the surface of iron–carbon[13,14] or bi-metals.[15,16] This may be a promising way for the *in situ* generation of H_2O_2. However, ME processes with a low capacity of H_2O_2 generation due to the usage of unsuitable ME materials have limited the application. It has been reported that H_2O_2 could be generated by the reaction of Zn with O_2,[17–19] and the carbon nanotubes (CNTs) could improve the two-electron reduction of O_2 during an electrochemical reaction because of their good electrical conductivity, high surface activity and mechanical strength.[20,21] Therefore, it can be assumed that Zn-CNTs/O_2 micro-electrolysis may have a high capacity of H_2O_2 generation. Moreover, the Zn-CNTs/O_2 process has following advantages for Fenton degradation: (1) the active hydrogen [H] generated during the micro-electrolysis process has a high chemical activity;[13,22] (2) the regeneration of Fe^{3+} can be improved by Zn^0 and enables the maximal amount of ˙OH to be generated *via* the decompose of H_2O_2 by Fe^{2+}; (3) the freshly formed $Zn(OH)_2$ colloid through the reaction between Zn^{2+} and OH^- during the micro-electrolysis process has a good adsorption capacity for the pollutants. In this study, 4-chlorophenol was selected as the model pollutant to assess the efficiency of the proposed Zn-CNTs/O_2/Fe^{2+} system due to its high toxicity and extensive application.[23,24]

[a]*College of Chemistry and Materials Science, Sichuan Normal University, Chengdu 610066, PR China*

[b]*Collaborative Innovation Center for Advanced Nuclear Energy Technology, INET, Tsinghua University, Energy Science Building, Beijing 100084, PR China. E-mail: wangjl@tsinghua.edu.cn; Fax: +86-10-62771150; Tel: +86-10-62784843*

[c]*Beijing Key Laboratory of Radioactive Wastes Treatment, Tsinghua University, Beijing 100084, PR China*

The objective of this study was to investigate the *in situ* generation of H_2O_2 from the micro-electrolysis process and its use for the degradation of 4-chlorophenol. A Zn-CNT composite was prepared, characterized and used for the reduction of dissolved O_2 to generate H_2O_2. The generated H_2O_2 subsequently reacted with Fe^{2+}, forming Fenton's reagent that oxidizes contaminants in the wastewater. The degradation of 4-CP in the secondary effluent of a municipal wastewater treatment plant was studied to examine the effect of wastewater composition on 4-CP degradation. The intermediate products were detected and the possible degradation pathway of 4-CP and the reaction mechanism of the Zn-CNTs/O_2/Fe^{2+} process were tentatively proposed.

2. Materials and methods

2.1 Materials and chemicals

4-Chlorophenol (purity 99%) was reagent grade and purchased from Sigma-Aldrich. The solvents (acetonitrile) used to prepare the mobile phase for the chromatographic analyses were HPLC grade. Hydroxyl-containing multi-walled CNTs (d < 8 nm, l = 10–30 μm) was purchased from the Beijing Deke Daojing Nano-Company, China. Polyethylene glycol 4000 (PEG) was purchased from the National Medicines Corporation Ltd., China. Zinc powder was obtained from the Shandong Xiya Corporation Ltd., China. All the other chemicals used in this study were analytical grade from the National Medicines Corporation Ltd., China. All reagents were used without further purification. De-ionized water was used in all experiments.

2.2 Preparation and characterization of Zn-CNTs

The Zn-CNT particles were prepared as follows: zinc powder, multi-walled CNTs and 40% w polyethylene glycol 4000 (the mass ratio of Zn, CNTs and PEG was 3 : 1 : 2) were mixed, and then dried at room temperature to form a slurry. The obtained slurry was heated for 1 h at 550 °C in a pipe furnace with a N_2 flow rate of 60 mL min^{-1}, followed by slow cooling to room temperature.

The morphology of Zn-CNTs was observed by using a transmission electron microscope (TEM) (HRTEM, JEM2100 and JEOL). The specific surface areas (BET) and the Barrett–Joyner–Halenda (BJH) pore size distribution of Zn-CNTs were determined by nitrogen adsorption–desorption isotherm measurements. X-ray photoelectron spectroscopy (XPS) analysis was performed by using an Al Kα X-ray (1486.6 eV) source for the excitation (NOVA 3200e).

2.3 4-Chlorophenol degradation experiments

The degradation experiments were performed in a 0.5 L glass bottle containing 0.25 L of solution. Pure O_2 was fed with flow rate of 400 mL min^{-1} through a diffuser placed at the bottom of the reactor. To promote convection, a stirrer was placed in the reactor at a constant rate of 300 rpm. The reaction temperature was kept at 25 ± 1 °C. Prior to the experiment, the desired initial pH of the solution was adjusted using H_2SO_4 (0.1 M) and NaOH (0.1 M). The experiments were carried out in duplicate and the average results were used.

To evaluate the effect of wastewater composition on the degradation of 4-CP, the secondary effluent of a municipal wastewater treatment plant spiked with 4-CP (25 mg L^{-1} or 50 mg L^{-1}) was used. The secondary effluent of wastewater was collected at a local wastewater treatment plant (WWTP) and used as received within the next 2 days. The initial 4-CP and TOC of the secondary effluent were 0 mg L^{-1} and 9.17 ± 1 mg L^{-1}, respectively.

2.4 Chemical analyses

4-CP was analyzed by HPLC, equipped with an XDB-C18 (4.6 × 150 mm) reversed-phase column and a diode array detector (DAD). The mobile phase was prepared with water and acetonitrile with a flow rate of 1 mL min^{-1}. The ratio (v/v) was 40/60. H_2O_2 was determined by a UV-Vis Spectrophotometry (PerkinElmer Lambda 25) at a wavelength of 385 nm. Total organic carbon (TOC) was measured using a TOC/TN analyzer (2100, Analytik Jena, Germany).

The intermediate products were identified by HPLC-MS equipped with the above-mentioned column coupled to a Shimadzu 2010EV mass spectrometer with an ESI ion source (LC-MS 2010, Columbia, USA). It was equipped with a photo diode array (PDA) detector, and operated in a negative mode. The analysis of the intermediate products was performed under the aforementioned solvent conditions. The injected volume was 30 μL. The organic acids were determined by ion-exclusion chromatography.

3. Results and discussion

3.1 Characterization of Zn-CNT composites

A typical TEM images of the newly prepared Zn-CNTs and the used Zn-CNTs are presented in Fig. 1, which reveals that the Zn-CNTs possessed a skeletal network of CNTs with some particles adhered to the surface of CNTs. Fig. 1(b) shows that the surface of the used Zn-CNT composite was covered by some large aggregates, indicating the formation of precipitates during the degradation of 4-CP by the Zn-CNTs/O_2/Fe^{2+} system.

Fig. 2 illustrates the N_2 adsorption–desorption isotherms and BJH pore size distribution plots, which were determined from the adsorption branch of the N_2 isotherms for the newly prepared and the used Zn-CNTs. The isotherms were identified as type IV and the hysteresis loops as type H3, which are the characteristics of mesoporous materials and have a slit pore of plate structure.

The pore-size distribution obtained from the isotherm indicated that most of the pores were in the range 2 to 10 nm, and the average pore size was calculated to be 17 nm and 14 nm for the newly prepared and the used Zn-CNT composites, respectively. The BET specific surface areas were calculated from N_2 isotherms, and were about 27 m^2 g^{-1} and 63 m^2 g^{-1} for the newly prepared and the used Zn-CNTs, respectively. The total pore volume was 0.12 cm^3 g^{-1} for the newly prepared Zn-CNTs and 0.23 cm^3 g^{-1} for the used Zn-CNTs. The extremely

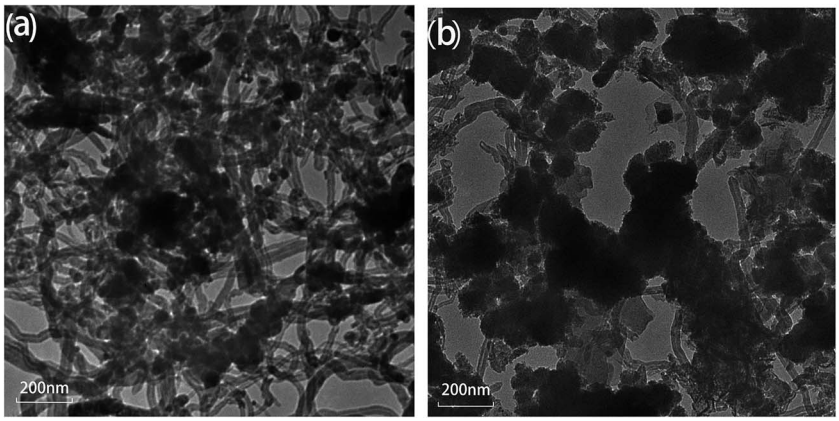

Fig. 1 TEM images of the newly prepared Zn-CNTs (a) and the used Zn-CNTs (b).

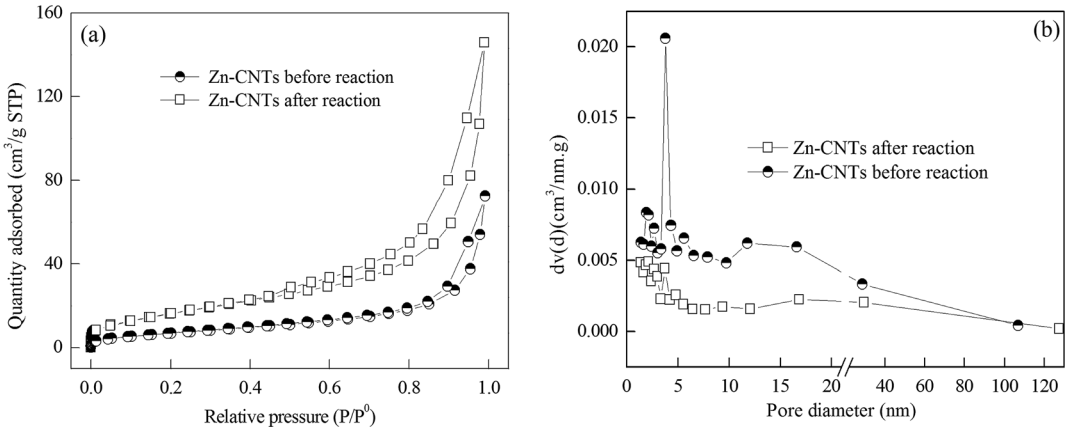

Fig. 2 N_2 adsorption/desorption isotherms and pore size distributions of the newly prepared Zn-CNTs (a) and the used Zn-CNTs (b).

high BET surface area and large total pore volume strongly supported the fact that Zn-CNT composite had a porous structure, which was consistent with the result of the TEM images. Compared with the newly prepared Zn-CNTs, the increase of the BET specific surface area and total volume of the pores for the used Zn-CNTs may be due to the formation of small pores caused by the corrosion of zinc and the deposition of zinc oxide on the surface of Zn-CNTs during the reaction between Zn-CNTs and oxygen. The similar average pore size of the newly prepared Zn-CNTs and the used Zn-CNTs indicated that the pores of the Zn-CNTs were not seriously blocked by the formed precipitates during the reaction.

Surface analysis of the newly prepared Zn-CNTs and the used Zn-CNTs was carried out using XPS (Fig. 3). The peaks for O 1s and O KLL were observed at 529.6 and 995.0 eV, respectively. Additional peaks (525.9 and 535.4 eV) for Zn 2p indicated different chemical environments. The peak for C 1s at approximately 284.8 eV was observed. Compared with the newly prepared Zn-CNTs, Fe 2p peaks were observed, indicating that a lot of iron was deposited on the surface of the Zn-CNTs after the reaction of Zn-CNTs with Fe^{2+}.

Fig. 3(b) and (c) exhibit the Auger KE of Zn in the newly prepared and the used Zn-CNT composites. From the standard data, the Auger KE of Zn^0 was about 992.1 eV, while ZnO was at 987.7–988.5 eV. Thus, the peak at 991.7 eV could be assigned to Zn^0,[25] and the peak at 988.5 eV could be assigned to ZnO.[26] Compared with the newly prepared Zn-CNTs, the peak at 986.4 eV was assigned to $Zn(OH)_2$,[27] which was observed for the used Zn-CNTs, demonstrating the interaction between Zn^{2+} and OH^- species. The formation of $Zn(OH)_2$ was consistent with the result of the TEM analysis. The Fe state in the used Zn-CNTs is shown in Fig. 3(d). The coexistence of Fe(0), Fe(I) and Fe(II) was evidenced by four shoulders. The main peak at 717.9 eV was assigned to the Fe(0) species.[28] The higher binding energy Fe $2p_{3/2}$ peak at 710.7 eV and its shake-up satellites at 724.3 eV ($2p_{1/2}$) were reported for Fe_3O_4.[29] The peak at 712.5 eV corresponds to a satellite transition that is the characteristic feature of Fe^{2+},[30] indicating that the interaction occurred between Zn^0, Fe^{2+} and the oxidant.

3.2 *In situ* generation of H_2O_2 in the Zn-CNTs/O_2 system

The variation of H_2O_2 concentration *versus* the reaction time at different initial pH values is shown in Fig. 4.

It was noted that at the initial pHs of 2.0 and pH 6.0, the reaction of Zn-CNTs with O_2 led to the formation of H_2O_2 and

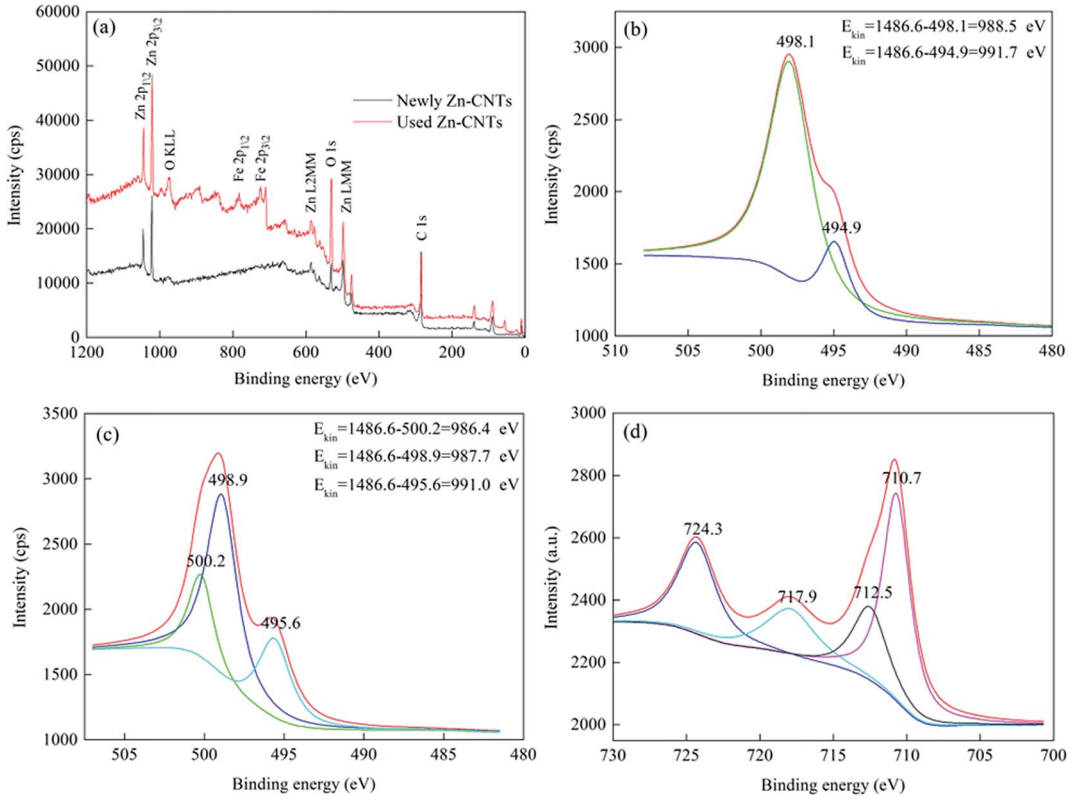

Fig. 3 XPS full survey spectra (a), Zn Auger KE spectra of the newly prepared Zn-CNTs (b), Zn Auger KE spectra of the used Zn-CNTs (c), Fe 2p spectra of the used Zn-CNTs (d).

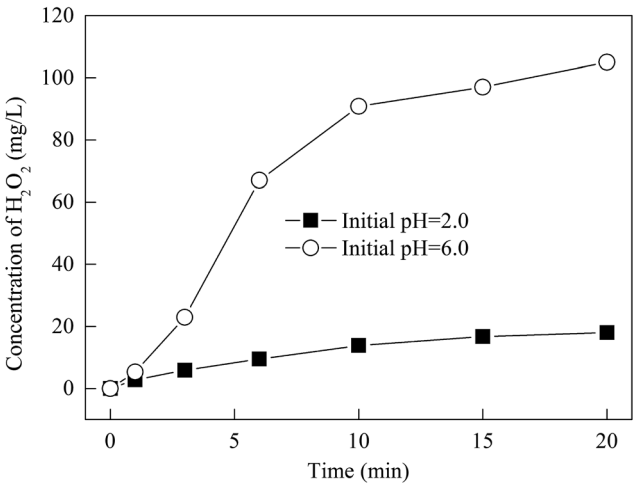

Fig. 4 Variation of H_2O_2 concentration with reaction time at different initial pH values. Experimental conditions: O_2 flow rate = 400 mL min^{-1}, [Zn-CNTs] = 2.0 g L^{-1}, T = 25 °C.

the concentration of H_2O_2 increased with reaction time. The concentration of H_2O_2 within 20 min was 19.5 and 103 mg L^{-1} at the initial pHs of 2.0 and 6.0, respectively. The formation of H_2O_2 was due to the micro-electrolysis process. In Zn-CNTs, Zn^0 adhered to the surface of the CNTs and the numerous corrosion cells were formed between Zn^0 particles and CNTs when they contacted wastewater. If dissolved O_2 existed in the solution, H_2O_2 was generated due to the reduction of O_2 in the cathode of the Zn^0-CNT corrosion cells and the reactions are listed as follows (eqn (1)–(3)):

Anode:

$$Zn - 2e^- \rightarrow Zn^{2+} \quad (1)$$

Cathode:

$$O_2 + 2H^+ + 2e^- \rightarrow H_2O_2 \quad (2)$$

$$2H^+ + 2e^- \rightarrow H_2 \quad (3)$$

In the acid solution, the competition of the reduction between H^+ and O_2 (shown in eqn (3)) led to a lower concentration of accumulated H_2O_2 at an initial pH of 2.0 than at an initial pH of 6.0.

It was reported that a certain concentration of H_2O_2 was found in the Zn^0/O_2 or Al^0/O_2 systems. However, the concentration of the generated H_2O_2 in the Zn^0/O_2 system was below 18 mg L^{-1} with a stoichiometry of the same dosage as that of Zn in a neutral solution.[17–19] In the Al^0/O_2 process, the concentration of H_2O_2 was only 180 μM at an Al^0 dosage of 5.0 g L^{-1} and reaction time of 250 min.[15] Therefore, the *in situ* generation of H_2O_2 can be improved by the electrode reaction in the corrosion cell with Zn^0 as the anode and the

CNTs as the cathode, which favored the two-electron reduction of O_2.

3.3 Degradation and mineralization of 4-CP in different systems

To investigate the catalytic performance of the Zn-CNTs/O_2 system for the degradation of 4-CP by Fenton oxidation, 4-CP degradation experiments in aqueous solution were carried out in different systems, including Zn-CNTs/O_2, Fe^{2+}/H_2O_2 and Zn-CNTs/O_2/Fe^{2+}. The removal efficiencies for 4-CP and TOC with reaction time are shown in Fig. 5. As depicted in Fig. 5(a), the removal efficiencies of 4-CP in Zn-CNTs/O_2, Fe^{2+}/H_2O_2 and Zn-CNTs/O_2/Fe^{2+} systems were 15.57%, 45.50% and 98.8% after 20 min of reaction at initial pH 2.0, respectively.

Fig. 5(b) shows that neither the Zn-CNTs/O_2 nor the Fe^{2+}/H_2O_2 system was efficient for TOC removal, with only 14.0% and 9.94% of TOC removed, respectively, after 20 min of reaction. Compared with the Zn-CNTs/O_2 and Fe^{2+}/H_2O_2 systems, the Zn-CNTs/O_2/Fe^{2+} system led to an 87.4% TOC removal within 20 min, which clearly indicated that the combination of Zn-CNTs/O_2 and Fe^{2+} had a synergetic effect. The 4-CP removal efficiency was quite similar to the TOC removal efficiency in the Zn-CNTs/O_2 system, suggesting that a low degradation of 4-CP occurred in the Zn-CNTs/O_2 system and the removal of 4-CP in the Zn-CNTs/O_2 process was due to the adsorption of 4-CP by Zn-CNTs, which exhibited an excellent adsorption capacity for 4-CP and enhanced its degradation.

Therefore, the Zn-CNTs/O_2/Fe^{2+} system is one of the most efficient electrochemical AOPs, consistent with the continuous production of $^{\cdot}OH$ using Fenton oxidation with micro-electrolysis generated H_2O_2. The oxidation mechanisms of the Fenton oxidation process are shown in the following equations:

$$O_2 + 2H^+ + 2e^- \rightarrow H_2O_2 \quad (4)$$

$$H_2O_2 + Fe^{2+} \rightarrow Fe^{3+} + OH^- + {}^{\cdot}OH \quad (5)$$

$$Fe^{3+} + H_2O_2 \rightarrow Fe^{2+} + HO_2^{\cdot} + H^+ \quad (6)$$

$$2Fe^{3+} + Zn \rightarrow 2Fe^{2+} + Zn^{2+} \quad (7)$$

It was reported that the rate of reaction (5) (k = 63–76 M^{-1} s^{-1}) was more rapid than that of reaction (6) (k = (0.1–1.0) × 10^{-2} M^{-1} s^{-1}), and the oxidative capability of $^{\cdot}OH$ was higher than that of $HO_2^{\cdot}$.[31,32] So, the regeneration of Fe^{2+} from Fe^{3+} played a key role in increasing the degradation rate of 4-CP by the Fenton oxidation process.[33,34] In the Zn-CNTs/O_2/Fe^{2+} process, the regeneration of the catalytic species (Fe^{2+} ions) was expected to occur *via* reactions (6) and (7). The regeneration of Fe^{2+} could be obtained from the intensification reduction of Fe^{3+} by Zn (eqn (6)), which produced enough Fe^{2+} to catalyze the H_2O_2 dissociation, which increased the mineralization rate of the pollutants. This was one of the reasons for the higher degradation efficiency of 4-CP in the Zn-CNTs/O_2/Fe^{2+} system than in the Fe^{2+}/H_2O_2 system. Moreover, in the Zn-CNTs/O_2/Fe^{2+} system, the dissolved oxygen could improve the production of the *ortho–para* chlorophenolperoxyl radical (ClPP$^{\cdot}$) and increase the extent of benzene ring cleavage. Therefore, 4-CP degradation in the Fenton/O_2 system was better than that in the Fenton/N_2 system.[35,36]

The high concentration of H_2O_2, the rapid regeneration of Fe^{2+} from the reduction of Fe^{3+} by Zn and the good adsorption capability of Zn-CNTs for 4-CP all contributed to the higher oxidative capability of the Zn-CNTs/O_2/Fe^{2+} system. It was reported that 50 mg L^{-1} of 4-CP was completely degraded after 2 h in the bimetallic Al–Fe/O_2 process, while after 20 min in the Zn-CNTs/O_2/Fe^{2+} process, many active intermediate species of H_2O_2 could be generated.[16] This result proved the effectiveness of the Zn-CNTs/O_2/Fe^{2+} process, which might be a promising alternative for the degradation of recalcitrant organic pollutants in wastewaters.

3.4 Involved active species

tert-Butanol (TBA) is known as an $^{\cdot}OH$ scavenger, which are widely used to examine the role of $^{\cdot}OH$. As shown in Fig. 6, the 4-CP removal efficiency decreased obviously when TBA was added to Zn-CNTs/O_2/Fe^{2+} system, indicating that 4-CP was mainly decomposed by the attack of $^{\cdot}OH$ (including surface-bound $^{\cdot}OH$ and free $^{\cdot}OH$). The iodide ion is used to scavenge the surface-bounded $^{\cdot}OH$.[21,37,38] It can be seen that the removal efficiency

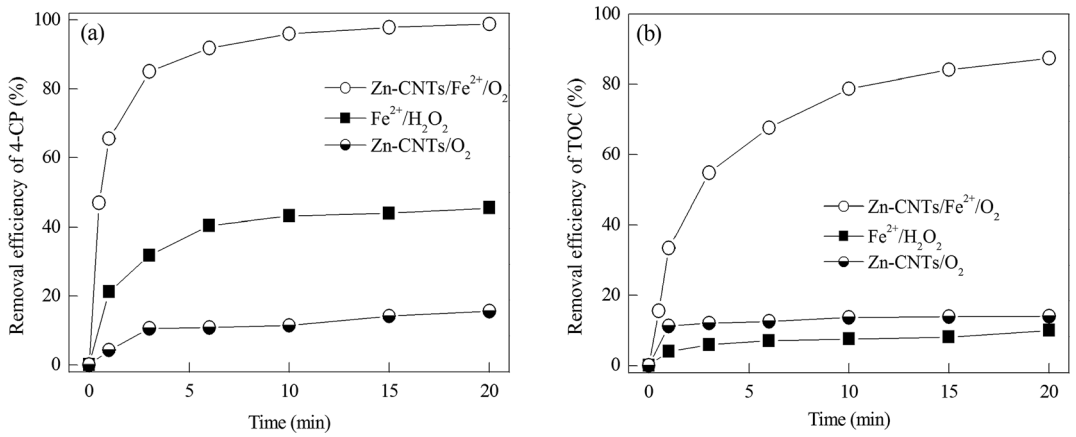

Fig. 5 Comparison of 4-CP degradation in different reaction systems. Experimental conditions: $[4\text{-CP}]_0$ = 50 mg L^{-1}, O_2 flow rate = 400 mL min^{-1}, [Zn-CNTs] = 2.0 g L^{-1}, $[Fe^{2+}]$ = 20 mg L^{-1}, $[H_2O_2]$ = 20 mg L^{-1}, T = 25 °C, pH = 2.0.

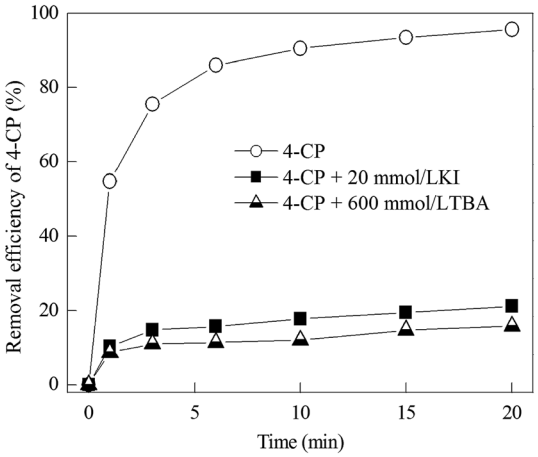

Fig. 6 Effect of radical scavengers on the degradation of 4-CP. Experimental conditions: $[4\text{-CP}]_0$ = 50 mg L^{-1}, O_2 flow rate = 400 mL min^{-1}, [Zn-CNTs] = 2.0 g L^{-1}, $[Fe^{2+}]$ = 20 mg L^{-1}, T = 25 °C, pH = 2.0.

of 4-CP was only 21.2% in 20 min when excess KI (20 mmol L^{-1}) was added into the system, which was lower than that of the system without scavengers (98.8% removal efficiency of 4-CP). This suggested that surface-bound ˙OH played a significant role in the degradation of 4-CP. The inhibited degree of the two scavengers was similar, indicating that the degradation of 4-CP was primarily attributed to the surface bound ˙OH.

3.5 Influencing factors for 4-CP degradation

3.5.1 Effect of the initial pH. pH is an important parameter for the generation of H_2O_2 by the reduction of O_2 on the surface of Zn-CNTs (Fig. 4), and pH also affects the dominant iron species in aqueous solution and the generation of ˙OH through the Fenton processes. The influence of the initial pH on the degradation of 4-CP by the Zn-CNTs/O_2/Fe^{2+} process was investigated (Fig. 7). With the decrease of initial pH from 4.0 to 3.0, the removal efficiency of 4-CP increased from 50.2% to 86.6% within 20 min. The removal efficiency of 4-CP was 91.4% at an initial pH of 1.0, which was slightly lower than at an initial pH of 2.0 after 20 min of reaction. The best degradation performance was achieved at an initial pH of 2.0, with 98.8% degradation within 20 min of reaction. The increased degradation efficiency at a lower pH was attributed to the higher oxidation potential of ˙OH and the higher stability of H_2O_2 in an acidic solution, which could not immediately decompose to H_2O and O_2.[8,33]

In order to explain the effect of the initial pH on the removal efficiency of 4-CP, the variation of pH during the Zn-CNTs/O_2/Fe^{2+} process was determined and is shown in Fig. 7(b). It was noted that the pH value increased gradually to be stable with a prolonged reaction time. The final pH was 2.1, 5.0, 5.3 and 6.6,

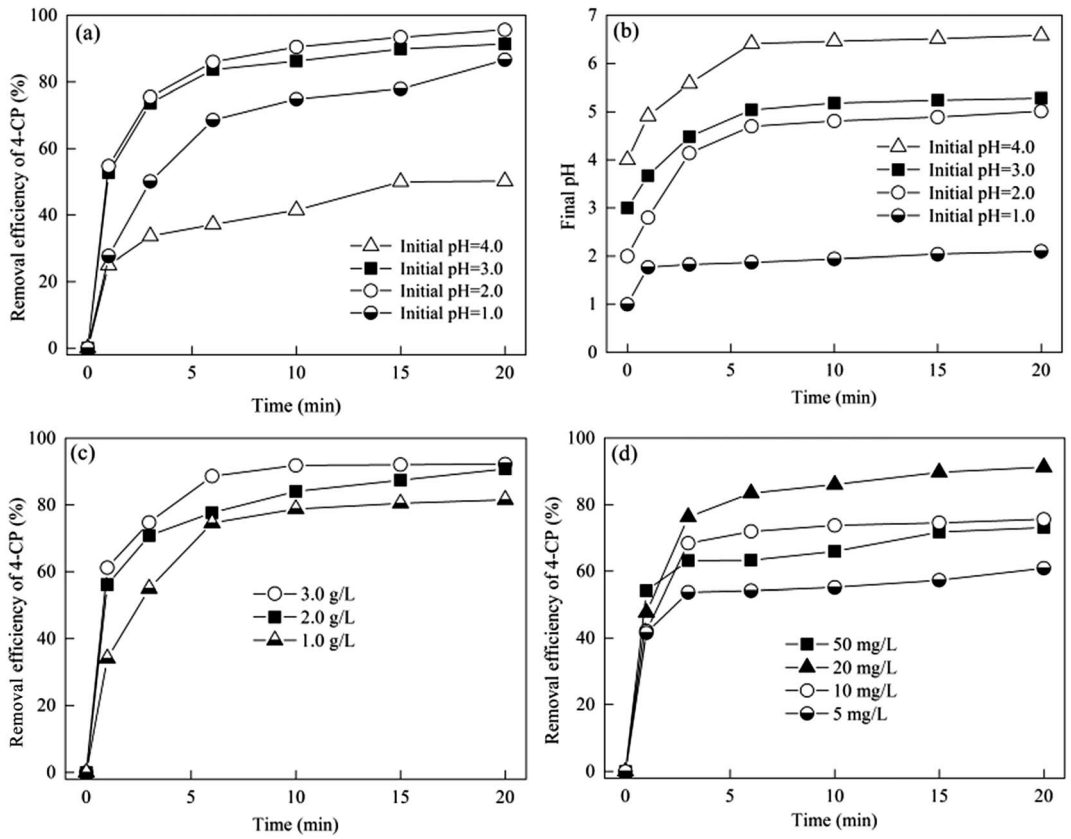

Fig. 7 Influencing factors for 4-CP degradation in the Zn-CNTs/O_2/Fe^{2+} system: (a) initial pH; (b) the variation of the solution pH; (c) Zn-CNTs dosage; (d) Fe^{2+} concentration. Except for the investigated parameters, other parameters were fixed: $[4\text{-CP}]_0$ = 50 mg L^{-1}, O_2 flow rate = 400 mL min^{-1}, [Zn-CNTs] = 2.0 g L^{-1}, $[Fe^{2+}]$ = 20 mg L^{-1}, T = 25 °C, pH = 2.0.

respectively, when the initial pH was 1.0, 2.0, 3.0 and 4.0, respectively. Several processes performed simultaneously in the Zn-CNTs/O_2/Fe^{2+} system, including the hydrolysis of the Zn(II) species or the Fe(III) species, the production of small-molecule organic acids, and the generation of H_2O_2 or H_2 by the reduction of O_2 or H^+. H^+ was released into the solution in the first two processes and consumed in the third process. At the beginning, the generation rate of H_2O_2 or H_2 was faster than the consumption rate of H^+, which led to the increase of pH. When the generation rate of H^+ was equal to its consumption rate, the solution pH was kept stable in a relative narrow range. This variation trend of the solution pH during the Zn-CNTs/O_2/Fe^{2+} process could lead to a low pH environment for pollutant degradation and high pH conditions for neutralization without chemical addition, which is an important advantage for its practical application.

3.5.2 Effect of Zn-CNTs dosage. The Zn-CNTs dosage will affect the concentration of H_2O_2 in solution, which controlled the productivity of $^{\bullet}OH$. The effect of Zn-CNTs dosage on 4-CP degradation was investigated. It can be observed that degradation of 4-CP increased with the increase of Zn-CNTs dosage. However, when the dosage of Zn-CNTs was higher than 2.0 g L^{-1}, the degradation of 4-CP was not significantly increased, possibly because higher Zn-CNTs dosage generated more H_2O_2 in solution, and excess H_2O_2 might also be converted to $HO_2^{\bullet}$ instead of $^{\bullet}OH$ because of scavenging effect of $^{\bullet}OH$ by H_2O_2.[39]

$$^{\bullet}OH + H_2O_2 \rightarrow HO_2^{\bullet}/O_2^{\bullet -} + H_2O \quad (8)$$

As shown in reaction (8), if H_2O_2 was excess, a less oxidative radicals ($HO_2^{\bullet}$ and $O_2^{\bullet -}$) might be produced and a highly oxidative radical ($^{\bullet}OH$) was consumed.[40,41] The optimal Zn-CNTs dosage was 2.0 g L^{-1} in this experiment.

3.5.3 Effect of Fe^{2+} concentration. The effect of Fe^{2+} concentration on the degradation of 4-CP is illustrated in Fig. 7(d). It can be observed that the 4-CP removal efficiency was low (only 60.9%) at an Fe^{2+} concentration of 5 mg L^{-1}. When the Fe^{2+} concentration increased to 10 mg L^{-1} and 20 mg L^{-1}, the 4-CP removal efficiency was 75.6% and 98.8%, respectively. This can be explained by the Fenton reaction (9), in which Fe^{2+} ions promoted H_2O_2 decomposition and increased the production of $^{\bullet}OH$. Fig. 7(d) also shows that when the Fe^{2+} concentration was increased from 20 mg L^{-1} to 50 mg L^{-1}, the 4-CP removal efficiency decreased from 98.3% to 73.5%, suggesting that an excess of iron was detrimental to the degradation of 4-CP because excess iron would consume $^{\bullet}OH$ (eqn (10)) and reduce the amount of available Fe^{2+} ion to catalyze H_2O_2 dissociation.[7] Hence, for the effective degradation of 4-CP, the Fe^{2+} concentration was 20 mg L^{-1}.

$$Fe^{2+} + H_2O_2 \rightarrow Fe^{3+} + {}^{\bullet}OH \quad (9)$$

$$Fe^{2+} + {}^{\bullet}OH \rightarrow Fe^{3+} + OH^- \quad (10)$$

3.6 Degradation of 4-CP in actual wastewater

The degradation of 4-CP in the secondary effluent spiked with 4-CP is given in Fig. 8. It can be seen that the removal efficiencies of 4-CP and TOC in the secondary effluent spiked with 50 mg L^{-1} 4-CP were 47.0% and 45.6%, respectively. The removal efficiencies of 4-CP and TOC in the secondary effluent were lower than that of the previous experiments in aqueous solution at the same conditions, in which 98.8% and 87.7% of 4-CP and TOC were removed (Fig. 5). The reason may be due to the presence of typical constituents, such as Cl^-, SO_4^{2-}, HPO_4^{2-} and HCO_3^-, anions in the secondary effluent, which can act as $^{\bullet}OH$ scavengers and retard the Fenton reaction.[42] Nevertheless, the removal efficiency of TOC was over 45% in the secondary effluent with two different concentrations of 4-CP, suggesting that the Zn-CNTs/O_2/Fe^{2+} process was very effective for the advanced treatment to remove persistent organic pollutants such as 4-CP in municipal wastewater.

3.7 The intermediate products and pathway of 4-CP degradation

The variation of the concentration of formic, acetic and oxalic acids during the degradation of 4-CP is illustrated in Fig. 9. As can be seen, the concentration of formic and oxalic acids began to increase within 5 min, reached a peak at about 6 min, and then decreased. Additionally, the concentration of acetic acid was very low, below 1 mg L^{-1} within 20 min.

The intermediate products generated during the 4-CP degradation process by the Zn-CNTs/O_2/Fe^{2+} system were determined by LC-MS analysis. Intermediates at *m*/*z* 143, *m*/*z* 191 and *m*/*z* 195 were observed in the aqueous phase, which indicated that the substitution reaction of $^{\bullet}OH$ and the addition reaction of $^{\bullet}OH$ were involved in the Zn-CNTs/O_2/Fe^{2+} process. The appearance of intermediates at *m*/*z* 199 and *m*/*z* 91 suggested the occurrence of the opening ring of aromatics and dehalogenation in the degradation process. The intermediate at *m*/*z* 189 might be the oxidized product of the intermediate at *m*/*z* 199 by O_2. Benzoquinone (BQ) was not detected, which indicated that the direct dechlorination of 4-CP by $^{\bullet}OH$ attack could

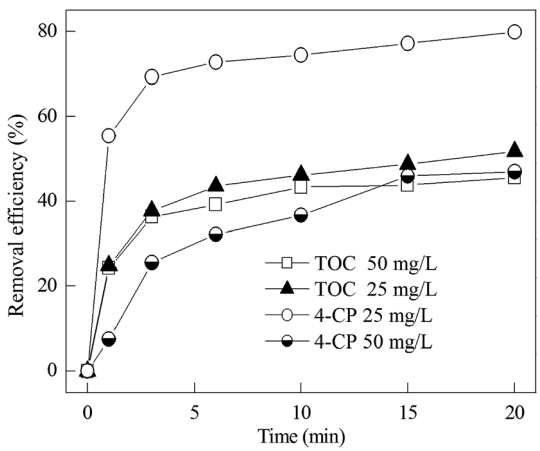

Fig. 8 Effect of wastewater composition on the degradation of 4-CP by the Zn-CNTs/O_2/Fe^{2+} system. Experimental conditions: O_2 flow rate = 400 mL min^{-1}, [Zn-CNTs] = 2.0 g L^{-1}, [Fe^{2+}] = 20 mg L^{-1}, T = 25 °C, pH = 2.0.

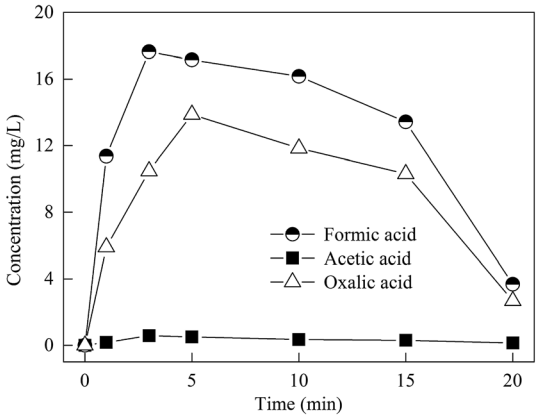

Fig. 9 Evolution of the concentration of small organic acids formed during the degradation of 4-CP. Experimental conditions: $[4\text{-CP}]_0$ = 50 mg L^{-1}, O_2 flow rate = 400 mL min^{-1}, [Zn-CNTs] = 2.0 g L^{-1}, $[Fe^{2+}]$ = 20 mg L^{-1}, T = 25 °C, pH = 2.0.

be neglected and 4-CP degradation was mainly by the 4-chlorocatechol (4CC) pathway in the Zn-CNTs/O_2/Fe^{2+} system.[23,35]

As a result, the main degradation pathway is proposed in Fig. 10. According to previous studies, 4-chlorocatechol was rapidly formed when the reaction was initiated by the attack of ·OH at the *ortho*-position of the hydroxyl group. 4-Chlorocatechol was attacked by the addition or substitution reaction of ·OH to form chlorinated intermediates D2 and D3. D2 can be easily transformed into quinine D5. Then, the C=C bond in the aromatic rings was cleaved by the attack of ·OH to yield D4 and D6, which were oxidized to aliphatic carboxylic acid intermediates (*e.g.*, formic acid, acetic acid, oxalic acid, *etc.*) that would be further mineralize into CO_2 and H_2O.

3.8 Reaction mechanism in the Zn-CNTs/O_2/Fe^{2+} system

On the basis of the aforementioned analyses and the Fenton oxidation mechanism,[8,20,31,43,44] the reaction mechanism of the Zn-CNTs/O_2/Fe^{2+} process is tentatively proposed (Fig. 11). In the

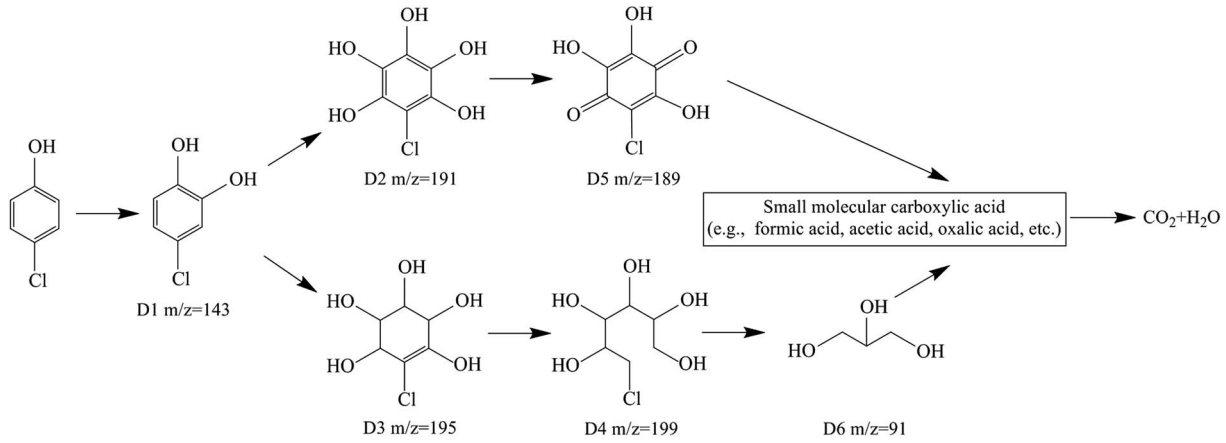

Fig. 10 Proposed degradation pathway of 4-CP by the Zn-CNTs/O_2/Fe^{2+} system.

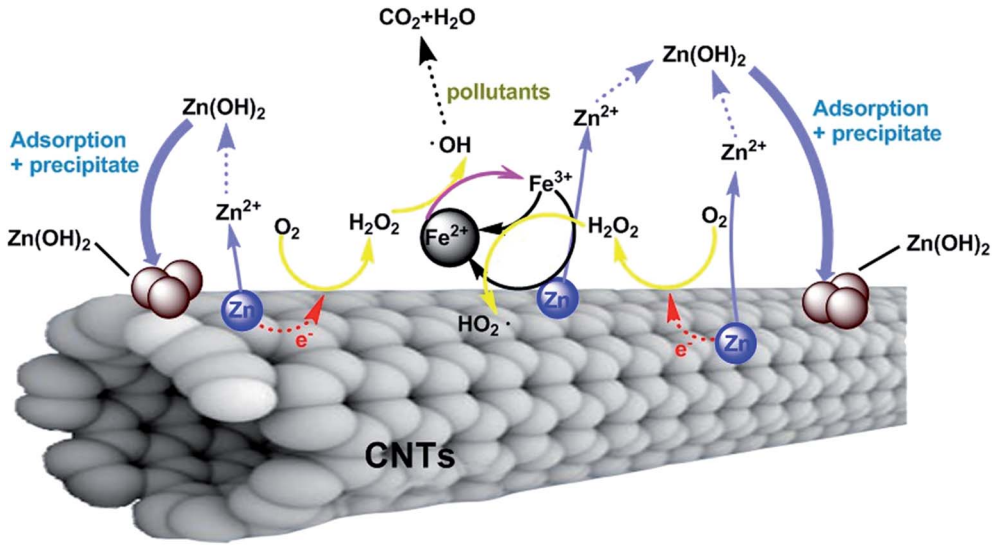

Fig. 11 The reaction mechanism of the Zn-CNTs/O_2/Fe^{2+} system.

Zn-CNT composite, Zn^0 adheres to the surface of the CNTs and numerous corrosion cells were formed between the particles of Zn^0 and CNTs, which was followed by reaction with dissolved O_2, leading to H_2O_2 formation. Then, surface chemisorbed H_2O_2 diffused onto the surface of Zn-CNTs or in the solution, and were decomposed into the $^{\bullet}OH$ radical by Fe^{2+}. In the last stage, the organic molecules approached the $^{\bullet}OH$ radical and were oxidized.

During the Zn-CNTs/O_2/Fe^{2+} process, the formed Fe^{3+} ions could be reduced to Fe^{2+} *via* reactions (6) and (7). The transformation of Fe^{3+} into Fe^{2+} was enhanced by Zn^0 in Zn-CNTs, which made enough Fe^{2+} to catalyze the H_2O_2 dissociation and improve the Fenton process.

Zn is classified as a low toxicity metal, and a very small amount of Zn^{2+} remained in the aqueous solution at the end of the reaction. During the Zn-CNTs/O_2/F $^{2+}$ process, Zn^{2+} in solution could be converted into the low solubility $Zn(OH)_2$ with a solubility product constant of 1.2×10^{-17} at pH 7 and 25 °C *via* the combination with the OH^- generated due to the reduction of H^+ and O_2 (Fig. 7). Therefore, the secondary pollution of Zn^{2+} could be avoided. The newly formed $Zn(OH)_2$ colloids with large specific surface areas had a high adsorption capacity for pollutants and improved the removal of pollutants.

The Zn-CNTs/O_2/Fe^{2+} system was developed in this study in order to *in situ* generate H_2O_2 and directly supply it to the Fenton reaction, because H_2O_2 is not stable, and it is not convenient to transport and store it for practical industrial applications. The preparation of Zn-CNTs was very simple and could be easily scaled up, which makes the Zn-CNTs/O_2/Fe^{2+} system available for large-scale wastewater treatment. In the Zn-CNTs/O_2/Fe^{2+} system, CNTs were not consumed during the wastewater treatment; although H_2O_2 is an inexpensive chemical and CNTs may be expensive, the cost of wastewater treatment using this system should be evaluated compared to the conventional Fenton process in the future.

4. Conclusions

In this paper, Zn-CNT composites were prepared and applied for the degradation of 4-CP by using a micro-electrolysis (MF)-Fenton system, in which the *in situ* generation of H_2O_2 was achieved through a two-electron reduction of oxygen on the surface of the Zn-CNTs. During the Zn-CNTs/O_2/Fe^{2+} process, the degradation of 4-CP was achieved due to the *in situ* generation of a high concentration of H_2O_2, the rapid regeneration of Fe^{2+} from the reduction of Fe^{3+} by Zn and the high adsorption capability of the Zn-CNT composite for pollutants. At an Fe^{2+} concentration of 20 mg L^{-1}, initial pH of 2.0, Zn-CNT dosage of 2.0 g L^{-1}, reaction time of 20 min and O_2 flow rate of 400 mL min^{-1}, the removal efficiencies of 4-CP and TOC were 98.8% and 87.3%, respectively, when initial 4-CP concentration was 50 mg L^{-1}.

Conflicts of interest

There are no conflicts to declare.

Acknowledgements

This research was supported by the National Natural Science Foundation of China (51338005) and the Program for Changjiang Scholars and Innovative Research Team in the University (IRT-13026).

References

1 J. L. Wang and Z. Y. Bai, *Chem. Eng. J.*, 2017, **312**, 79–98.
2 J. L. Wang and L. B. Chu, *Radiat. Phys. Chem.*, 2016, **125**, 56–64.
3 J. L. Wang and L. J. Xu, *Crit. Rev. Environ. Sci. Technol.*, 2012, **42**, 251–325.
4 M. S. Yalfani, S. Contreras, J. Llorca, M. Dominguez, J. E. Sueiras and F. Medina, *Phys. Chem. Chem. Phys.*, 2010, **12**, 14673–14676.
5 M. S. Yalfani, S. Contreras, F. Medina and J. E. Sueiras, *J. Hazard. Mater.*, 2011, **192**, 340–346.
6 S. Yuan, Y. Fan, Y. Zhang, M. Tong and P. Liao, *Environ. Sci. Technol.*, 2011, **45**, 8514–8520.
7 G. Santana-Martínez, G. Roa-Morales, E. Martin Del Campo, R. Romero, B. A. Frontana-Uribe and R. Natividad, *Electrochim. Acta*, 2016, **195**, 246–256.
8 Y. Liu, S. Chen, X. Quan, H. Yu, H. Zhao and Y. Zhang, *Environ. Sci. Technol.*, 2015, **49**, 13528–13533.
9 Y. Zhang, L. Ma, J. Li and Y. Yu, *Environ. Sci. Technol.*, 2007, **41**, 6264–6269.
10 L. Clarizia, D. Russo, I. Di Somma, R. Marotta and R. Andreozzi, *Appl. Catal., B*, 2017, **209**, 358–371.
11 L. Zhuang, S. Zhou, Y. Li, T. Liu and D. Huang, *J. Power Sources*, 2010, **195**, 1379–1382.
12 L. Fu, S. You, G. Zhang, F. Yang and X. Fang, *Chem. Eng. J.*, 2010, **160**, 164–169.
13 Q. Zhu, S. Guo, C. Guo, D. Dai, X. Jiao, T. Ma and J. Chen, *Chem. Eng. J.*, 2014, **255**, 535–540.
14 S. Zhang, D. Wang, L. Zhou, X. Zhang, P. Fan and X. Quan, *Chem. Eng. J.*, 2013, **217**, 99–107.
15 J. Fan, X. Liu and L. Ma, *Chem. Eng. J.*, 2015, **263**, 71–82.
16 X. Liu, J. Fan and L. Ma, *Chem. Eng. J.*, 2014, **236**, 274–284.
17 G. Wen, S. Wang, J. Ma, T. Huang, Z. Liu, L. Zhao and J. Su, *J. Hazard. Mater.*, 2014, **265**, 69–78.
18 Y. Li, L. Yang, C. Chen and Y. Lan, *Water, Air, Soil Pollut.*, 2016, **227**, 364–382.
19 J. Zhang, Y. Wu, L. Liu and Y. Lan, *Sep. Purif. Technol.*, 2015, **151**, 318–323.
20 Z. Ai, T. Mei, J. Liu, J. Li, F. Jia, L. Zhang and J. Qiu, *J. Phys. Chem. C*, 2007, **111**, 14799–14803.
21 S. Mukherjee, A. Bates, S. C. Lee, D. H. Lee and S. Park, *Int. J. Green Energy*, 2015, **12**, 787–809.
22 R. Chen, L. Chai, Y. Wang, H. Liu, Y. Shu and J. Zhao, *Trans. Nonferrous Met. Soc. China*, 2012, **22**, 983–990.
23 T. Zhou, Y. Li, J. Ji, F. Wong and X. Lu, *Sep. Purif. Technol.*, 2008, **62**, 551–558.
24 W. S. Kuo and L. N. Wu, *Sol. Energy*, 2010, **84**, 59–65.
25 W. L. Dai, Q. Sun, J. F. Deng, D. Wu and Y. H. Sun, *Appl. Surf. Sci.*, 2001, **177**, 172–179.

26 A. C. Hegde, K. Venkatakrishna and N. Eliaz, *Surf. Coat. Technol.*, 2010, **205**, 2031–2041.
27 K. Pohl, J. Otte, P. Thissen, M. Giza, M. Maxisch, B. Schuhmacher and G. Grundmeier, *Surf. Coat. Technol.*, 2013, **218**, 99–107.
28 X. Song, Q. Shi, H. Wang, S. Liu, C. Tai and Z. Bian, *Appl. Catal., B*, 2017, **203**, 442–451.
29 T. Yamashita and P. Hayes, *Appl. Surf. Sci.*, 2008, **254**, 2441–2449.
30 V. P. S. Awana, Govind, A. Pal, B. Gahtori, S. D. Kaushik, A. Vajpayee, J. Kumar and H. Kishan, *J. Appl. Phys.*, 2011, **109**, 3296–32997.
31 G. B. Ortiz De La Plata, O. M. Alfano and A. E. Cassano, *Appl. Catal., B*, 2010, **95**, 1–13.
32 A. D. Bokare and W. Choi, *J. Hazard. Mater.*, 2014, **275**, 121–135.
33 L. Zhang, H. Zeng, Y. Zeng, Z. Zhang and X. Zhao, *J. Mol. Catal. A: Chem.*, 2014, **392**, 202–207.
34 B. G. Kwon, D. S. Lee, N. Kang and J. Yoon, *Water Res.*, 1999, **33**, 2110–2118.
35 Y. Du, M. Zhou and L. Lei, *J. Hazard. Mater.*, 2007, **139**, 108–115.
36 Y. Du, M. Zhou and L. Lei, *Water Res.*, 2007, **41**, 1121–1133.
37 L. Xu and J. Wang, *J. Hazard. Mater.*, 2011, **186**, 256–264.
38 Z. Wan and J. Wang, *J. Hazard. Mater.*, 2017, **324**, 653–664.
39 M. Hou, L. Liao, W. Zhang, X. Tang, H. Wan and G. Yin, *Chemosphere*, 2011, **83**, 1279–1283.
40 F. Duan, Y. Yang, Y. Li, H. Cao, Y. Wang and Y. Zhang, *Journal of Environmental Sciences*, 2014, **26**, 1171–1179.
41 H. Chen, L. Zhang, H. Zeng, D. Yin, Q. Zhai, X. Zhao and J. Li, *J. Mol. Catal. A: Chem.*, 2015, **406**, 72–77.
42 E. Lipczynska Kochany, G. Sprah and S. Harms, *Chemosphere*, 1999, **30**, 9–20.
43 G. B. Ortiz De La Plata, O. M. Alfano and A. E. Cassano, *Appl. Catal., B*, 2010, **95**, 14–25.
44 G. B. Ortiz De La Plata, O. M. Alfano and A. E. Cassano, *J. Photochem. Photobiol., A*, 2012, **233**, 53–59.